

Full Length Research Paper

# A molecular Redox Sensor from *Streptomyces rimosus* M4018 for *Escherichia coli*

Zhenyu Tang<sup>1</sup>, Yingping Zhuang<sup>1</sup>, Ju Chu<sup>1</sup>, Siliang Zhang<sup>1</sup>, Paul Herron<sup>2</sup>, Iain S. Hunter<sup>2</sup> and Meijin Guo<sup>1\*</sup>

<sup>1</sup>State Key Laboratory of Bioreactor Engineering, East China University of Science and Technology, Shanghai 200237, P.R. China.

<sup>2</sup>Strathclyde Institute of Pharmacy and Biomedical Sciences, University of Strathclyde, Glasgow, G4 0re, Scotland, United Kingdom.

Accepted 22 November, 2011

In order to enable microorganisms to manifest their intracellular oxygen levels we constructed a genetic sensor circuitry which converts signals impinging on the cellular redox balance into a reporter gene expression readout. Based on the newly found *Streptomyces rimosus* redox control system, consisting of Rex modulating Retinopathy of prematurity (ROP)-containing promoters in a NADH-dependent manner, we designed an *Escherichia coli* sensor transcription control system, which constitutes a Rex transactivator (REDOX) with the ability to bind and activate promoters. When oxygen levels were high and resulted in depleted NADH pools, Rex-specific target promoter (*cydP1*) driven from the expression of secreted (Green fluorescent protein, GFP) reporter gene was low as a consequence of increased Rex-ROP affinity. Conversely, at hypoxic conditions, it led to high intracellular NADH levels, strongly reduced Rex-ROP interaction and increased GFP expression in *E. coli* cells. The sensor capacity (oxygen levels) of redox system enabled monitoring of the population's metabolic state *in vivo*. Our research will not only help to understand the molecular mechanism of the Rex family but also foster progresses in biosensor development.

**Key words:** *Streptomyces rimosus* M4018, Rex operator, Redox sensor.

## INTRODUCTION

Nicotinamide adenine dinucleotide (NAD<sup>+</sup>) and its reduced form, NADH, are found in all living cells. The NADH/NAD<sup>+</sup> ratio reflect both the metabolic activities and the health of cells (Schafer and Buettner, 2001). NADH can be utilized in the cytosol and mitochondria (Gladden, 2004; Ren et al., 1988; Rowell and Shepherd, 1996; Sahlin, et al., 1987; Yamada, et al., 2006) to maintain the redox states (NADH/NAD<sup>+</sup>), which play an important role in metabolic regulation (Graham and Saltin, 1989; Zhou et al., 2005; 2006). Since NAD<sup>+</sup> and NADH participate in both energy metabolism and non-redox cellular

pathways, it is necessary to monitor the cellular NADH/NAD<sup>+</sup> ratio simultaneously in order to give a true picture of how cells respond to environmental stimuli.

Several methods are currently available for the determination of NAD<sup>+</sup> and NADH in cells and tissues, such as fluorescence imaging (Kasischke et al., 2004), enzymatic assay (Dekoning and Vandam, 1992), high-performance liquid chromatography (Yamada et al., 2006), and electrospray ionization mass spectrometry (ESI-MS) (Sadanaga-Akiyoshi et al., 2003). However, these methods can not measure the redox states (NADH and NAD<sup>+</sup> or NADH/NAD<sup>+</sup> ratio) distinctly in cytosol and mitochondria or their transport fluxes *in vivo*.

Rex (redox regulator) was initially characterized in *Streptomyces coelicolor* and is the first transcriptional regulator that responds directly to the balance of the

\*Corresponding author. E-mail: [guo\\_mj@ecust.edu.cn](mailto:guo_mj@ecust.edu.cn). Tel: +86 21 64251131. Fax: +86 21 64253702.

NADH/NAD<sup>+</sup> redox system (Brekasis and Paget, 2003). In *S. coelicolor*, Rex controls not only the expression of the cytochrome bd terminal oxidase operon (*cydABCD*) but also its own transcription. Oxygen limitation can rapidly induce the transcription of the *cydABCD* operon. An inverted repeat sequence known as ROP (Rex operator) is recognized as the Rex binding site. Recently, Sr-Rex was characterized in *Streptomyces rimosus* M4018 (Shen et al., 2011). Previous studies have shown that both NAD<sup>+</sup> and NADH have affinity to Rex, but only the NADH-Rex complex causes Rex to lose its affinity for deoxyribonucleic acid (DNA). As a result, the NADH/NAD<sup>+</sup> ratio can be monitored by means of the binding of NADH for the pyridine-binding site and be reflected by the Rex repressor activity. This in turn can be used in the characterization of the electrons flow through the respiratory chain and the oxygen availability. Weber et al. (2006) engineered the *S. coelicolor* Rex protein as a specific nutrient and oxygen sensor, which was able to report the metabolic state of transgenic CHO cells grown in serum-free suspension cultures. As a novel mechanism of sensing the intracellular redox state, the NADH/NAD<sup>+</sup>-sensing mechanism of Rex family members currently remains unknown. Once understood, however, it may provide insights for other redox-sensing proteins whose functions are regulated by the intracellular NADH/NAD<sup>+</sup> ratio.

The increase in oxygen, decreases intracellular NADH pools by enhancing oxidative phosphorylation, therefore the NADH/NAD<sup>+</sup> ratio is closely related to the oxygen levels. In this study, we engineered the *S. rimosus* Rex protein as a specific oxygen sensor, which is able to report the metabolic state of *Escherichia coli* cells. Our research will help to understand the molecular mechanism of the Rex family and also foster advances in the development *in vivo* biosensors.

## MATERIALS AND METHODS

### Bacterial strains, media, and plasmids

*E. coli* strains DH5 $\alpha$  and BL21 (DE3) were used for routine subcloning and protein expression, respectively. Organisms were grown at 37°C in Luria-Bertani (LB) medium (1% Tryptone, 1% NaCl, 0.5% yeast extract), and standard procedures were used for transformation (Sambrook et al., 1989). *E. coli* transformants were selected with apramycin (50  $\mu$ g ml<sup>-1</sup>) or kanamycin (50  $\mu$ g ml<sup>-1</sup>). The cloning vectors used were pMD19-T (TaKaRa), pET28a (*In vitro*gen), pPIC3.5K-(Green fluorescent protein, GFP) (Xiulin Qin, East China University of Science and Technology) and pOJ446 (Iain S. Hunter, University of Strathclyde). *S. rimosus* M4018 (Petkovic et al., 2006) was grown and manipulated as described previously (Kieser et al., 2000).

### Cloning of Sr-Rex and Retinopathy of prematurity (ROP)

Genomic DNA was isolated from cultures of *S. rimosus* M4018, as previously described (Kieser et al., 2000). Primers were designed based on the available sequence of *rex* in *S. rimosus* (*Sr-rex*).

Forward primer *rex*F (5'-GGGAATTCGTGGCAACTGGCCGA

GCACACC-3') was designed to incorporate an *Eco* RI restriction site (underlined); the reverse primer *rex*R (5'-GGGAAGCTTTCAGTGGTGGTGGTGGTGGTGGTGC CGGCATCACG-3') included a *Hind*III restriction site (underlined) and a hexahistidine-tag (double underlined), thus allowing cloning into a pET28a vector.

Because ROP exists in the promoter of cytochrome bd terminal oxidase (*cydP1*) in *S. coelicolor*, using forward primer ROPF (5'-TGTGAATGTGAAC GCGTTCACAAGC-3') and reverse primer ROPR (5'-TCTTCATCGGCTGC TGCTCGTACAT-3'), we amplified the whole *cydP1* and partial *cyd* gene and cloned them into pMD19-T vector to give pMD19-T-ROP. The PCR product was further confirmed by sequencing. Biotinylated ROP was produced by PCR-mediated ROP amplification from pMD19-T-ROP using primers ROPF-BIOTIN (5'-BIOTIN-TGTGAACGCGTTCACA -3') and ROPR (Figure 1b).

### Overexpression of Sr-Rex

The amplified Sr-Rex was restriction-digested with *Eco* RI/*Hin* dIII and ligated into the pET28a vector. It resulted in a phage T7 promoter (PT7)-driven expression vector (pET28a-Rex) for hexahistidine-tagged Sr-Rex production in *E. coli* BL21 (E-Rex). The transformed cells were used for overnight precultures, which were inoculated into 50 ml LB medium supplemented with 50  $\mu$ g ml<sup>-1</sup> kanamycin. The cells were incubated at 37°C, up to an OD<sub>600nm</sub> = 0.5. Then 1 mM isopropyl-1-thio- $\beta$ -D-galactopyranoside (IPTG) was added to induce the expression of T7 RNA polymerase. In order to determine the optimum period of induction, incubation of the flasks at 37°C was continued after the addition of IPTG to the fermentation broths and samples were taken every hour to determine the amount of Sr-Rex. The samples were then processed as followed: (1) centrifuge cultures, (2) resuspension of the pellets with 2 ml PBS, (3) sonicated for 2 min, (4) spinning the sonicated lysate and (5) the use of the supernatant for SDS-PAGE analysis. With the increase of induction time, its expression quantity increased, and when it was induced up to 5 h, the expression quantity peaked. The molecular weight of this protein was about 37 kDa.

### SDS-PAGE analysis of Sr-Rex

A 12% polyacrylamide gel was prepared for SDS-PAGE analysis. A 20  $\mu$ L aliquot of each sample was transferred to a fresh microcentrifuge tube, to which 5  $\mu$ L of 6  $\times$  loading dye had been added. The samples were mixed, boiled for two minutes, and then loaded onto the polyacrylamide gel. The gel was run for 120 min at 120 V and stained using Coomassie Blue R-250. The resulting gel was scanned for subsequent visual analysis.

### Purification of Sr-Rex

Cells (growth in LB medium) were harvested by centrifugation (16,000 g; 4°C; 15 min), and the pellet was resuspended in buffer A (20 mM Tris-HCl, 30 mM NaCl, pH 8.0). Then, the cells were broken through ultrasonication. The extract was loaded onto a Ni<sup>2+</sup> affinity column equilibrated with buffer A. The column was eluted stepwise with 100, 500 and 1000 mM imidazole in buffer A. The active fractions were collected and analyzed by SDS-PAGE. The purified proteins were used for further studies.

### *In vitro* characterization of Rex: ROP interaction

NADH-responsive interaction between Sr-Rex and ROP was

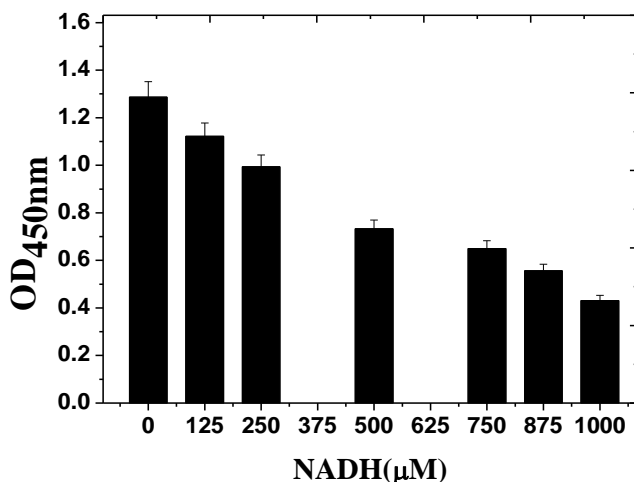


**Figure 1.** NADH-adjustable Rex-ROP binding characteristics. Biotinylated ROP was immobilized on streptavidin-coated microtiter plates and incubated with *Sr-Rex* in the presence of different NADH concentrations followed by a washing step for removal of unbound *Sr-Rex*. ROP-immobilized *Sr-Rex* was detected using a primary antibody specific for the hexahistidine-tag of *Sr-Rex* and a secondary horseradish peroxidase-conjugated antibody for colorimetric detection using 3,3',5,5'-tetramethylbenzidine (TMB).

performed using an ELISA-like setup, as described previously (Weber et al., 2005).

#### Construction of a redox biosensor in *E. coli*

##### **The construction of the *Sr-Rex* expression vector pET28a-Rex is described below:**

The Rex-specific target promoter (*cydP1*) was constructed by total gene biosynthesis and then cloned into the vector pBluescript II SK(+) to give pBlue-cydP1. The *gfp* gene was obtained from the pPIC3.5K-GFP vector using the oligonucleotides *gfpF* (5'-GGGGAATTCTGAACG CGTTCACATCAAC-3', where *Eco* RI is underlined, and the annealing sequence is in lower case) and *gfpR* (5'-GGGAAGCTTTTAC TTGTACAGCTCGTCC-3', *Hin* dIII underlined, annealing sequence in lower case). The amplified fragment was digested with *Eco* RI and *Hin* dIII and ligated with pBlue-cydP1, which was digested with the same restriction enzymes and resulted in pBlue-cydP1-GFP. The plasmid was digested with *Bam* HI and *Spe* I, and the fragment *cydP1*-GFP was cloned into the corresponding sites (*Bam* HI/*Spe* I) of pOJ446, thus resulting in a *cydP1*-driven GFP expression unit (pOJ446-GFP). It was then transformed into *E. coli* BL21 to give the E-GFP strain.

The two vectors pET28a-Rex and pOJ446-GFP were sequentially transformed into *E. coli* BL21 to yield a redox biosensor in *E. coli*. The new strain was designated as E-Redox.

#### Cell culture conditions and analytical assays

E-Redox cells were cultivated in LB medium, while E-Rex was used as the negative control and E-GFP acted as positive control. *Sr-Rex* was determined by SDS-PAGE, while green fluorescent

protein (GFP) expression was analyzed by fluorescence microscope and flow cytometry. GFP analysis was carried out using the futures commission merchant (FCM) method (Hohenblum et al., 2003), based on the fact that GFP can exhibit green fluorescence. After being diluted to  $1 \times 10^7$  cells  $\text{ml}^{-1}$  with phosphate-buffered saline, a 1 ml sample was analyzed on a FACScalibur (Becton Dickinson, Franklin Lakes, NJ). The cells were excited at 488 nm and the emission was detected using a 510 nm BP filter for GFP. Intracellular NADH concentrations were analyzed using the method as previously described (Menzel et al., 1998).

## RESULTS

### The binding activity of *Sr-Rex* and ROP *in vitro*

The NADH-adjustable ROP binding activity of *Sr-Rex* was demonstrated by assessing the *Sr-Rex*/ROP interaction in the presence of increasing NADH concentrations using an ELISA-like setup *in vitro*. The increase of NADH can be measured at OD<sub>450nm</sub>. As shown in Figure 1, more NADH was added, less OD<sub>450nm</sub> was detected. This is due to the fact that NADH can abolish the binding between *Sr-Rex* and ROP.

### Design of a Rex-derived *E. coli* expression system

The previous ELISA-like results showed the responsiveness of *Sr-Rex* to NADH concentration changes *in vitro*. To address whether it can project its

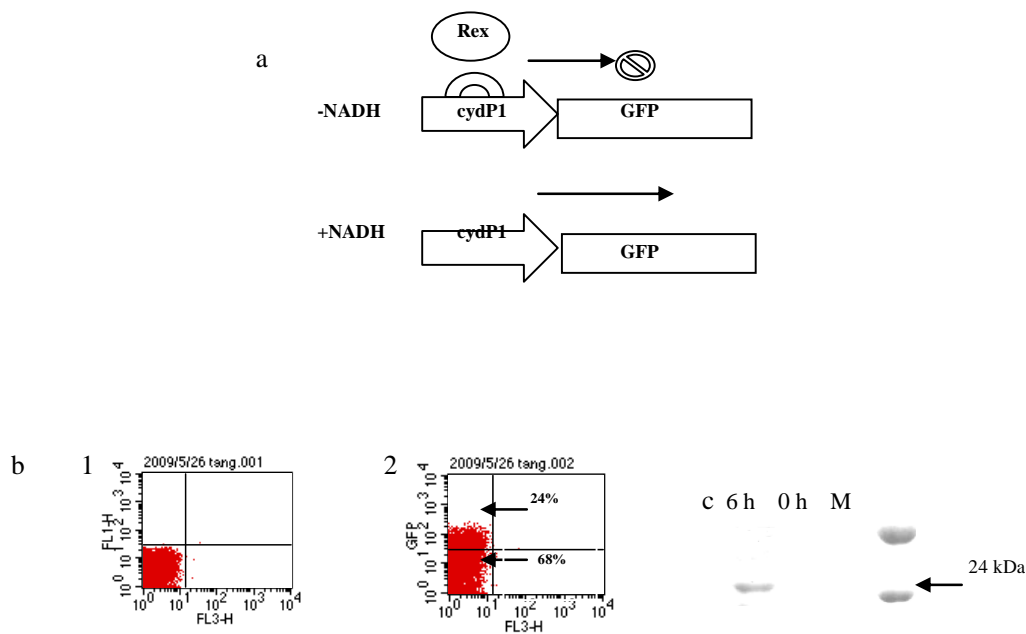


**Figure 2.** Design and function of the redox sensor for *E. coli*. (a) Function of the redox system. At low NADH levels (-NADH) *Sr-Rex* binds to *Sr-ROP* and represses the expression of GFP. At high NADH levels (+NADH), *Rex-ROP* binding is abolished which results in GFP expression. (b) Flow cytometry analysis of GFP expression in (1) negative control: E-rer; (2) positive control: E-GFP. Reporter expression was analyzed 6 h after fermentation. The x and y axes are in log scale and represent the viability of the cells and GFP expression, respectively. The percentage of GFP<sup>+</sup> cells is indicated in the plot. (c) SDS-PAGE analysis of GFP expression in E-GFP.

capacity to provide readout for physiological parameters that impact on intracellular NADH concentrations *in vivo*, a genetic sensor circuitry was constructed which enabled precise profiling of the intracellular redox state in *E. coli*. The *Sr-Rex* expression vector is pET28a-Rex, which is able to depress the *cydP1* promoter harboring the *Sr-ROP* module (Figure 2a), depending on the redox state of the cell. In order to evaluate whether *Sr-Rex* retains its *Sr-ROP*-binding and *cydP1* activating capacities in *E. coli*, *E. coli* BL21 cells were co-/transformed with pET28a-Rex and pOJ446-GFP or pOJ446-GFP alone. High GFP expression levels of E-GFP cells confirmed the efficiency of the *cydP1* promoter (Figure 2b to c).

### The redox sensor enables monitoring of oxygen deprivation in *E. coli*

Low intracellular oxygen concentrations are known to limit oxidative phosphorylation and thus to increase the intracellular NADH pool. E-Redox was cultivated in order to validate the redox sensor capacity. Fermentations were carried out with volumes of 50, 100 and 200 ml of LB medium, inoculated with the same cell concentration in standard 500 ml flasks. Presumably, with the smaller volumes of culture medium used in the culture experiments the rate of gaseous exchange between the

culture medium and the environment would be greater and would contain more dissolved oxygen, resulting in deprivation of the NADH pool. The GFP expression was profiled by flow cell cytometry (Figure 3a to e). Following the increase of the volume of the medium from 50 to 200 ml, the oxygen concentrations decreased and the NADH levels increased (Table 1), while the corresponding GFP levels increased as well (Figure 3). Furthermore, the presence of the GFP protein was confirmed by fluorescence microscopy (Figure 3h). Therefore, the redox sensor was able to sense the oxygen status of an *E. coli* cell culture as high oxygen levels correspond to low intracellular NADH concentrations, which intensifies the *Sr-Rex/ROP* interaction and thus results in low GFP expression levels. These data indicate that oxygen concentration changes are translated into significant NADH-mediated *Sr-Rex/ROP* transcription differences.

E-Redox was further analyzed without IPTG induction as well as under hypoxic condition followed by analysis of GFP expression. For the hypoxia conditions, oxygen was displaced from the flask by bubbling compressed N<sub>2</sub> through the culture and using the rubber stopper to seal the flask. The results showed that more GFP was expressed in 100 ml LB medium without IPTG induction (Figure 3f) than those found under IPTG induction condition (Figure 3d). This was due to the fact that no *Sr-Rex* protein was expressed without IPTG induction and

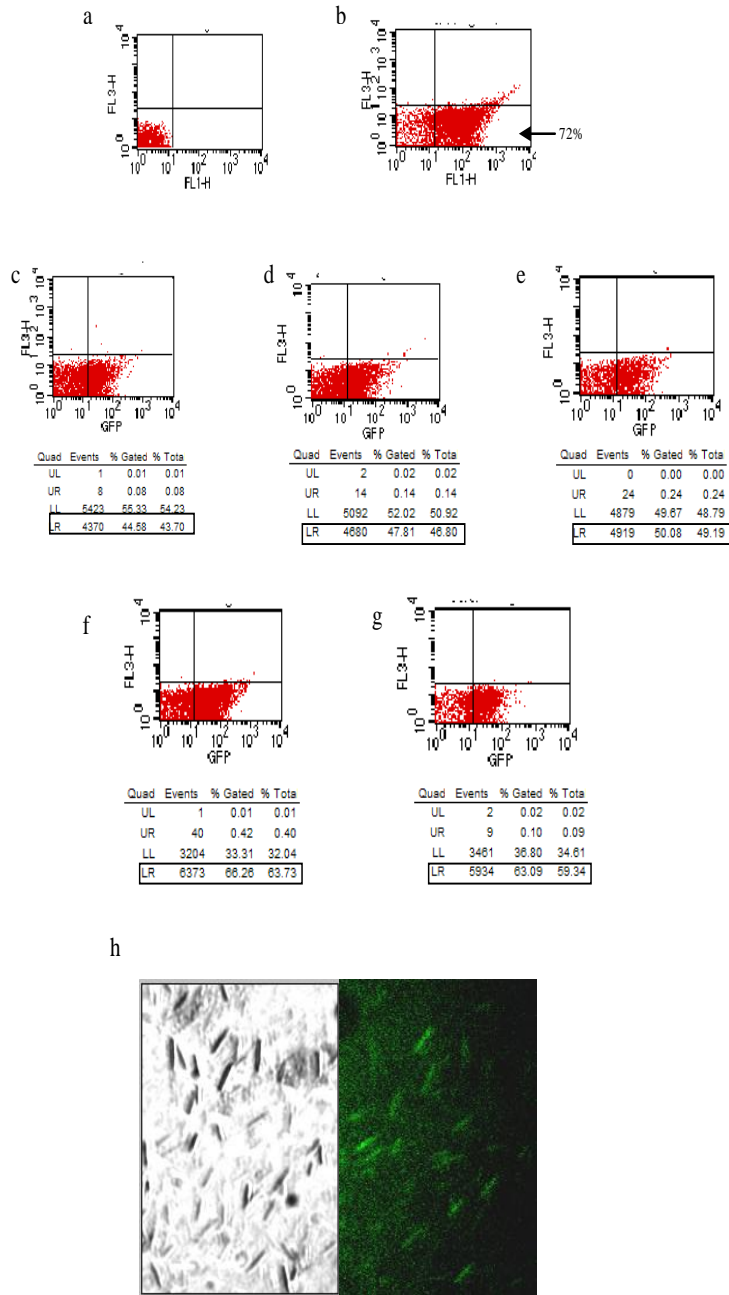


**Figure 3.** The redox sensor enables monitoring of oxygen deprivation in *E. coli*. (a-g): Flow cytometry analysis of GFP expression in (a) negative control: E-Rex in 50 ml LB medium with 0.5 mM IPTG induction, (b) positive control: E-GFP in 50 ml LB medium without IPTG induction, (c) E-Redox in 50 ml LB medium with 0.5 mM IPTG induction, (d) E-Redox in 100 ml LB medium with 0.5 mM IPTG induction, (e) E-Redox in 200 ml LB medium with 0.5 mM IPTG induction, (f) E-Redox in 100 ml LB medium without IPTG induction, (g) E-Redox in 100 ml LB medium under hypoxic conditions with 0.5 mM IPTG induction; Reporter expression was analyzed 6 hours after fermentation. The x and y axes are in log scale and represent the viability of the cells and GFP expression, respectively. The percentage of GFP<sup>+</sup> cells is indicated in the plot, (h) direct detection of GFP in E-Redox cultivated in 100 ml LB medium with 0.5 mM IPTG induction. Left: inverted microscope image; right: fluorescence microscope image.

**Table 1.** Intracellular NADH levels under different culture conditions.

	50 ml	100 ml	200 ml	100 ml (no IPTG)	100 ml (hypoxia)
NADH ( $\mu\text{mol/gDCW}$ )	1.6 $\pm$ 0.2	2.5 $\pm$ 0.3	4.2 $\pm$ 0.5	2.4 $\pm$ 0.2	5.3 $\pm$ 0.4

\*DCW: dry cell weight. Intracellular NADH levels under different culture conditions. Intracellular NADH concentrations were analyzed using the method as previously describes (Menzel et al., 1998). All analyses were conducted in triplicate.

could not form the Rex-ROP complex. Meanwhile, NADH-rich conditions such as hypoxia resulted in the depression of Rex-ROP interaction and more GFP was generated (Figure 3g). These observations document the suitability of the redox sensor reporter gene expression in *E. coli* cultures and recommend the genetic redox circuitry for monitoring of oxygen supplies in *E. coli*.

## DISCUSSION

### Comparison of Sr-Rex with Rex Family Members

Here we described the application of Sr-Rex, a novel redox-sensitive repressor in *S. rimosus* that appears to modulate transcription in response to changes in cellular NADH levels. The high degree of phylogenetic sequence conservation (Shen et al., 2011) suggests common structural mechanisms for redox-dependent gene regulation among Rex family members. The *S. rimosus* and *S. coelicolor* Rex homologs (S-Rex) share 84% sequence identity (Shen et al., 2011). So far, we have identified genes that encode Rex homologs in the sequenced genomes of most Gram-positive bacteria, including several important human and animal pathogens such as *Staphylococcus aureus* (Pagels et al., 2010). However, although Rex is found in the *Streptomyces* genus, it appears to be absent from other actinomycetes such as *Mycobacterium tuberculosis*. To date, no Rex homolog has been identified in Gram-negative bacteria, suggesting that Rex might be confined to Gram-positive organisms. Rex is predicted to include a Rossmann fold for pyridine nucleotide binding, and residues that might play key structural and nucleotide binding roles in this putative fold are highly conserved (Shen et al., 2011; Ellen et al., 2008). We propose therefore that Rex homologs are likely to act as regulatory sensors of NADH/NAD<sup>+</sup> redox poise in most Gram-positive bacteria.

### Sr-Rex DNA-binding activity is inhibited by NADH

Brekasis and Paget (2003) reported that the Sc-Rex protein, a novel sensor of the NADH/NAD<sup>+</sup> redox balance, binds to the *cis* elements of the *cyd* and *nuo* operons in *S. coelicolor*. Schau et al. (2004) determined the precise B-Rex (YdiH)-binding region in the *cyd* operon. In our previous study, Shen et al. (2011) gave

the first report which showed the presence of Rex in *S. rimosus*. It also demonstrated that NAD had no effect on the binding activity of Sr-Rex but NADH seemed to have a negligible effect or a partial negative effect on DNA-binding activity. With the increase in the medium volume from 50 ml to 200 ml, the NADH and the corresponding GFP levels increased, the former phenomenon was because the oxidative phosphorylation was diminished, while the latter was due to the fact that NADH can compete with ROP (*cydP1*) for the Rex binding, thus less Rex-ROP complex were formed in 200 ml culture condition and more GFPs were expressed (*cydP1* promoter had not been repressed). These data suggest that DNA-binding determinants of Sr-Rex are similar to those of Sc-Rex, where NADH completely inhibits its DNA-binding activity, but they are distinct from B-Rex, since in *B. subtilis* NAD<sup>+</sup> boosts the binding activity of Rex. The reason that NAD<sup>+</sup> fails to inhibit DNA-binding activity is either because NAD<sup>+</sup> can't bind to Rex or a NAD<sup>+</sup>+Rex complex competes with NADH for Rex binding. To test this, electrophoretic mobility shift assay (EMSA) are required that use a range of NADH concentrations in the presence of NAD<sup>+</sup>. Interestingly, B-Rex and Sc-Rex regulate respiratory metabolism gene expression via redox sensing of the NADH/NAD<sup>+</sup> ratio, although their DNA-binding determinants are distinct. Thus it seems likely that Sr-Rex can sense the NADH/NAD<sup>+</sup> redox balance as well.

### GFP-based redox biosensor is sensitive to oxygen levels in *E. coli*

Redox reactions pervade living cells. Therefore, precise assessment of the metabolic state of production cell lines is of pivotal importance for bioprocess development and cell-based therapies. Various regulatory sensors continually monitor the redox state of the internal and external environments and control the processes that work to maintain redox homeostasis. These sensors convert the redox signals into regulatory outputs, usually at the level of transcription, which allow the bacterium to adapt to the altered redox environment.

The Sr-Rex-based transcription circuitry, which shows sensitivity to oxygen levels, represents the genetic sensor system. This enables engineered production cell lines to directly monitor their metabolic state by the readout of certain reporter genes. Oxygen limitation is a major

parameter that compromises the growth and production of transgenic cell lines in biopharmaceutical manufacturing. In our study, the *Sr-Rex/Retinopathy of prematurity (ROP)* circuitry operated as expected in *E. coli* and managed secreted reporter gene expression in response to signals impinging on the cellular redox balance. We believe that the redox sensor converting the global metabolic state of *E. coli* into a reporter gene expression readout which will help to understand the molecular mechanism of the Rex family and also foster advances in the development in *in vivo* biosensors.

## ACKNOWLEDGEMENT

This work was supported by the Open Funding Project for State Key Laboratory of Bioreactor Engineering (No. 2060204), and National Basic Research Program of China (No. 2011CB200904).

## REFERENCES

- Brekasis D, Paget MS (2003). A novel sensor of NADH/NAD<sup>+</sup> redox poise in *Streptomyces coelicolor* A3(2): EMBO J., 22: 4856–4865.
- Dekoning W, Vandam KA (1992). Method for the determination of changes of glycolytic metabolites in yeast on a subsecond time scale using extraction at neutral pH. Anal. Biochem., 204: 118–123.
- Ellen W, Mikael CB, Annika R (2008). Structure and functional properties of the *Bacillus subtilis* transcriptional repressor Rex. Mol. Microbiol., 69(2): 466-478.
- Gladden LB (2004). Lactate metabolism: a new paradigm for the third millennium. J. Physiol., 558: 5–30.
- Graham TE, Saltin B (1989). Estimation of the mitochondrial redox state in human skeletal muscle during exercise. J. Appl. Physiol., 66: 561–566.
- Hohenblum H, Borth N, Mattanovich D (2003). Assessing viability and cell-associated product of recombinant protein producing *Pichia pastoris* with flow cytometry. J. Biotechnol., 102: 281–290.
- Kasischke KA, Vishwasrao HD, Fisher PJ (2004). Neural activity triggers neuronal oxidative metabolism followed by astrocytic glycolysis. Science, 305: 99–103.
- Kieser T, Bibb MJ, Buttner MJ, Chater KF, Hopwood DA (2000). Practical *Streptomyces* genetics. John Innes Foundation, Norwich, United Kingdom.
- Menzel K, Ahrens K, Zeng AP, Deckwer WD (1998). Kinetic, Dynamic, and Pathway Studies of Glycerol Metabolism by *Klebsiella pneumoniae* in Anaerobic Continuous Culture: III. Enzymes and Fluxes of Glycerol Dissimilation and 1,3-Propanediol Formation. Biotechnol. Bioeng., 59(5): 544-552.
- Pagels M, Fuchs S, Pané-Farré J, Kohler C, Menschner L, Hecker M, McNamara PJ, Bauer MC, von Wachenfeldt C, Liebeke M, Lalk M, Sander G, von Eiff C, Proctor RA, Engelmann S (2010). Redox sensing by a Rex-family repressor is involved in the regulation of anaerobic gene expression in *Staphylococcus aureus*. Mol. Microbiol., 76(5): 1142-1161.
- Petkovic H, Cullum J, Hranueli D, Hunter IS, Peric-Concha N, Pigac J, Thamchaipenet A, Vujaklija D, Long PF (2006). Genetics of *Streptomyces rimosus*, the Oxytetracycline Producer. Microbiol. Mol. Biol. Revs., 70: 704-728.
- Rowell LB, Shepherd (1996). Handbook of Physiology. Exercise: Regulation and Integration of Multiple Systems. Bethesda, MD: Am Physiol Soc., 12 (16): 705–769; 19: 870–911; 21: 952–994.
- Sadanaga-Akiyoshi F, Yao H, Tanuma S (2003). Nicotinamide attenuates focal ischemic brain injury in rats: with special reference to changes in nicotinamide and NAD<sup>+</sup> levels in ischemic core and penumbra. Neurochem. Res., 28: 1227–1234.
- Sahlin K, Katz A, Henriksson J (1987). Redox state and lactate accumulation in human skeletal muscle during dynamic exercise. Biochem. J., 245: 551–556.
- Sambrook J, Fritsch EF, Maniatis T (1989). Molecular cloning: a laboratory manual, 2nd ed. Cold Spring Harbor Press, Cold Spring Harbor, N.Y.
- Schafer F, Buettner G (2001). Redox environment of the cell as viewed through the redox state of the glutathione disulfide/glutathione couple. Free Radic. Biol. Med., 30: 1191–1212.
- Schau M, Chen Y, Hulett FM (2004). *Bacillus subtilis* YdiH is a direct negative regulator of the cydABCD operon. J. Bacteriol., 186: 4585–4595.
- Shen J, Tang ZY, Guo MJ, Zhang SL (2012). Cloning, Expression and Biological Function of *Sr-rex* Gene from *Streptomyces rimosus* M4018. Acta Microbiologica Sinica, 52(1): 30-35.
- Weber CC, Link N, Fux C, Zisch AH, Weber W, Fussenegger M (2005). Broad-spectrum protein biosensors for class-specific detection of antibiotics. Biotechnol. Bioeng., 89: 9–17.
- Weber W, Link N, Fussenegger M (2006). A genetic redox sensor for mammalian cells. Metab. Eng., 8: 273–280.
- Yamada K, Hara N, Shibata T (2006). The simultaneous measurement of nicotinamide adenine dinucleotide and related compounds by liquid chromatography/electrospray ionization tandem mass spectrometry. Anal. Biochem., 352: 282–285.
- Zhou L, Cabrera ME, Okere IC, Sharma N, Stanley WC (2006). Regulation of myocardial substrate metabolism during increased energy expenditure: insights from computational studies. Am. J. Physiol. Heart Circ. Physiol., 291: 1036–1046.
- Zhou L, Stanley WC, Saidel GM, Yu X, Cabrera ME (2005). Regulation of lactate production at the onset of ischaemia is independent of mitochondrial NADH/NAD<sup>+</sup>: insights from in silico studies. J. Physiol., 569: 925–937.